

Viscoelastic inhomogeneous beam under time-dependent strains: A longitudinal crack analysis

Victor I. Rizov*¹

*Department of Technical Mechanics, University of Architecture,
Civil Engineering and Geodesy, 1 Chr. Smimensky blvd., 1046 – Sofia, Bulgaria*

(Received August 4, 2020, Revised September 25, 2020, Accepted November 10, 2020)

Abstract. The present paper is concerned with analysis of two longitudinal cracks in a viscoelastic inhomogeneous cantilever beam. The loading of the beam is applied by two stages. At the first stage, the strains increase with time at a constant speed up to a given magnitude. At the second stage, the strains remain constant with time. The viscoelastic behavior of the beam is described by using a viscoelastic model with a linear spring in series with a linear dashpot and a second linear dashpot connected parallel to the spring and the first dashpot. Stress-strain-time relationships of the viscoelastic model are derived for both stages (at increasing strain and at constant strain with time). Time-dependent strain energy release rates are obtained for both longitudinal cracks by analyzing the balance of the energy. Solutions to the time-dependent strain energy release rate are derived also by considering the time-dependent strain energy stored in the beam structure. The solutions are used to analyze the change of the strain energy release rate with time at both stages of loading.

Keywords: longitudinal crack; viscoelastic beam; inhomogeneous material; time-dependent strain; analytical study

1. Introduction

The search for efficient decisions in various areas of the modern engineering very often leads to applications of continuously inhomogeneous structural materials. The most important characteristic of these materials is the fact that their properties vary continuously along one or more directions in the solid. Therefore, the material properties are continuous functions of one or more coordinates (Tokovyy and Ma 2017, Tokovyy and Ma 2019, Tokovyy 2019). The continuously inhomogeneous materials are very useful for load-bearing structural engineering applications in which different operational requirements are imposed on different parts of a structural member. This is due to the fact that the material properties of continuously inhomogeneous materials can be formed technologically by gradually changing the microstructure and composition during the manufacturing process. In this way, one can realize significant benefits from the continuous material inhomogeneity.

The functionally graded materials are a class of continuously inhomogeneous structural

*Corresponding author, Professor, E-mail: V_RIZOV_FHE@UACG.BG

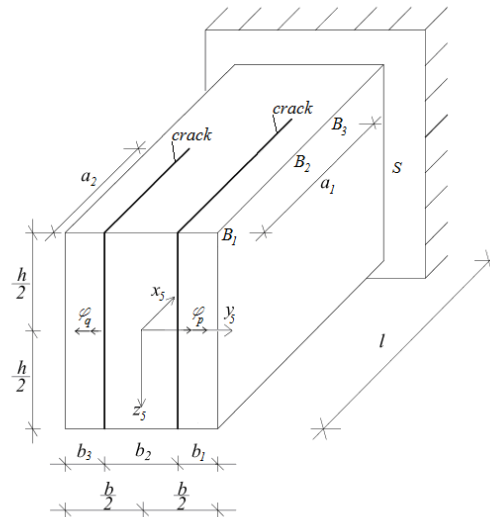


Fig. 1 Geometry of viscoelastic inhomogeneous cantilever beam with two longitudinal vertical cracks

materials which have attracted a considerable amount of attention throughout the world in the recent decades (Akbulut and Sonmez 2008, Akbulut *et al.* 2020, Altunsaray and Bayer 2014, Altunsaray 2017, Altunsaray *et al.* 2019, Butcher *et al.* 1999, Dolgov 2002, Gasik 2010, Hedia *et al.* 2014, Hirai and Chen 1999, Mahamood and Akinlabi 2017, Markworth *et al.* 1995, Miyamoto *et al.* 1999, Nemat-Allal *et al.* 2011, Rezaiee-Pajand and Hozhabrossadati 2016, Rezaiee-Pajand *et al.* 2017, Rezaiee-Pajand *et al.* 2018, Uslu Uysal and Kremzer 2015, Uslu Uysal 2016, Uslu Uysal and Güven, 2015). In fact, the functionally graded materials are new inhomogeneous composites made of two or more constituent materials. The ratios of the constituent materials vary smoothly in a functionally graded structural member (usually, across thickness).

The wide use of continuously inhomogeneous (functionally graded) materials in such important areas as aeronautical engineering, aerospace industry, nuclear power plants, car industry, electronics and biomedicine sets high requirements with regard to the fracture behavior of these novel composites (Dolgov 2005, Dolgov 2016, Uslu Uysal and Güven 2016). One of the significant crack problems is the longitudinal fracture of continuously inhomogeneous beam structures. This is due to the fact that continuously inhomogeneous (functionally graded) materials can be built up layer by layer (Mahamood and Akinlabi 2017, Markworth *et al.* 1995, Miyamoto *et al.* 1999) which is a premise for appearance of longitudinal cracks between layers. It should also be mentioned that beams are important structural members in various load-bearing engineering applications. Therefore, the problem of longitudinal fracture in continuously inhomogeneous beams is both of theoretical and practical interest.

The basic aim of the present paper is to derive solutions to the time-dependent strain energy release rate for two longitudinal vertical cracks in a viscoelastic inhomogeneous cantilever beam structure. It should be noted that the previous works on longitudinal fracture deal with obtaining of solutions to the strain energy release rates in continuously inhomogeneous beam configurations which do not exhibit viscoelastic behavior (Rizov 2017, Rizov 2018, Rizov 2020). A model with

one linear spring and two linear dashpots is used for describing the viscoelastic behavior of the inhomogeneous beam in the present paper. Solutions to the strain energy release rate are derived for two stages of loading. At the first stage, the strains increase with time at a constant speed. The strains remain constant with time at the second stage of loading. The change of the strain energy release rate with time at both stages of loading is evaluated by applying the solutions derived.

2. Viscoelastic model of inhomogeneous beam under time-dependent strains

The present analysis is focused on the inhomogeneous viscoelastic beam shown in Fig. 1. The cross-section of the beam is a rectangle of width, b , and height, h . The length of the beam is l . The beam is clamped in section, S . There are two longitudinal vertical cracks in the beam (Fig. 1). The lengths of the right-hand and left-hand cracks are denoted, respectively, by a_1 and a_2 where $a_1 > a_2$. The widths of the right-hand, interstitial and left-hand crack arms are b_1 , b_2 and b_3 , respectively. In portion, b_2+b_3 , the beam is divided by the right-hand crack in two crack arms (Fig. 1). The widths of the right-hand and left-hand crack arms in beam portion, B_2B_3 , are denoted, respectively, by b_1 and b_4 where $b_4=b_2+b_3$. The beam is loaded in pure bending at the free ends of the right-hand and left-hand crack arms so that the angles of rotation, φ_p and φ_q , of the free ends of the right-hand and left-hand crack arms increase with constant speeds, v_p and v_q , respectively, at $0 \leq t \leq t_1$.

$$\varphi_p = v_p t \tag{1}$$

$$\varphi_q = v_q t \tag{2}$$

where t is time.

At $t > t_1$, the two angles of rotation do not change with time

$$\varphi_p = v_p t_1 \tag{3}$$

$$\varphi_q = v_q t_1 \tag{4}$$

The interstitial crack arm is free of stresses (Fig. 1).

The beam under consideration exhibits linear viscoelastic behaviour that is described by using the model shown in Fig. 2. The model is a combination of a linear spring with modulus of elasticity, E , in series with a linear dashpot with coefficient of viscosity, η_Q , and a second linear dashpot with coefficient of viscosity, η_R , connected parallel to the spring and the first dashpot. In order to derive the stress-strain-time relationship for the viscoelastic model in Fig. 2, first, the equations for equilibrium of the components of the model are written as

$$\sigma_E + \sigma_R = \sigma \tag{5}$$

$$\sigma_Q + \sigma_R = \sigma \tag{6}$$

where, σ_E , σ_Q and σ_R are the stresses in the spring and in the dashpots with coefficients of viscosity, η_Q and η_R , respectively. The stresses are expressed as functions of strains by applying the Hooke's law.

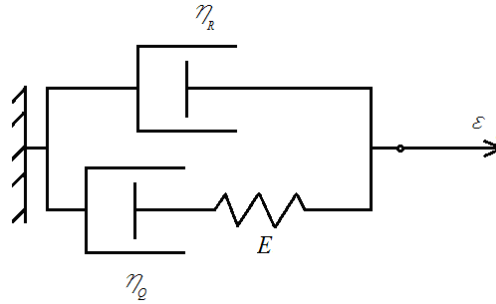


Fig. 2 Viscoelastic model

$$\sigma_E = E\varepsilon_E \quad (7)$$

$$\sigma_Q = \eta_Q \dot{\varepsilon}_Q \quad (8)$$

$$\sigma_R = \eta_R \dot{\varepsilon}_R \quad (9)$$

where, ε_E , ε_Q and ε_R are the strains in the spring and in the dashpots with coefficients of viscosity, η_Q and η_R , respectively.

The strains are related as (Fig. 2)

$$\varepsilon_E + \varepsilon_Q = \varepsilon \quad (10)$$

Besides

$$\varepsilon_R = \varepsilon \quad (11)$$

The strain, ε , increases with constant speed, v , at $0 \leq t \leq t_1$

$$\varepsilon = vt \quad (12)$$

By combining of (7) - (12), one obtains

$$\dot{\sigma} + \frac{E}{\eta_Q} \sigma = Ev \left(1 + \frac{\eta_R}{\eta_Q} \right) \quad (13)$$

The solution of (13) is found as

$$\sigma = \frac{\mu v}{\lambda} (1 - e^{-\lambda t}) \quad (14)$$

where

$$\lambda = \frac{E}{\eta_Q} \quad (15)$$

$$\mu = E \left(1 + \frac{\eta_R}{\eta_Q} \right) \quad (16)$$

By combining of (12) and (14), one derives the following stress-strain-time relationship:

$$\sigma = \frac{\mu \varepsilon}{\lambda t} (1 - e^{-\lambda t}) \quad (17)$$

At $t \geq t_1$, the strain, ε , is equal to νt_1 and does not change with time, i.e.

$$\varepsilon = \nu t_1 \quad (18)$$

By using of (7) - (11) and (18), one derives

$$\dot{\sigma} = -\frac{E}{\eta_Q} \sigma \quad (19)$$

The solution of (19) is obtained as

$$\sigma = \zeta \varepsilon e^{\frac{E}{\eta_Q}(t_1-t)} \quad (20)$$

where

$$\zeta = \frac{\mu}{\lambda t_1} (1 - e^{-\lambda t_1}) \quad (21)$$

Formula (21) is the stress-strain-time relationship at $t \geq t_1$.

The beam in Fig. 1 exhibits continuous material inhomogeneity along its height. The following exponential laws are used to describe the distributions of E , η_Q and η_R along the height of the beam:

$$E = E_0 e^{\frac{h+z_5}{h} f \frac{2}{h}} \quad (22)$$

$$\eta_Q = \eta_{Q_0} e^{\frac{h+z_5}{h} g \frac{2}{h}} \quad (23)$$

$$\eta_R = \eta_{R_0} e^{\frac{h+z_5}{h} r \frac{2}{h}} \quad (24)$$

where

$$-\frac{h}{2} \leq z_5 \leq \frac{h}{2} \quad (25)$$

In formulae (22) - (25), z_5 is the vertical centroidal axis of the beam cross-section, E_0 , η_{Q0} and

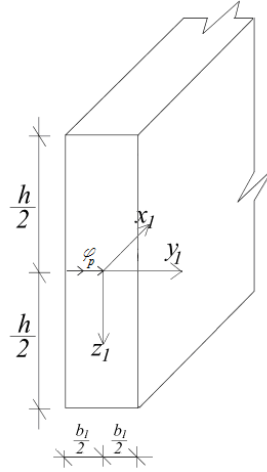


Fig. 3 Cross-section of the right-hand crack arm

η_{Q5} are the values of E , η_Q and η_R at the upper surfaces of the beam, respectively. The variations of E , η_Q and η_R along the height of the beam are controlled by the parameters, f , g and r , respectively.

3. Deriving the time-dependent strain energy release rate

The balance of the energy is analyzed in order to derive the time-dependent strain energy release rate for the longitudinal vertical cracks in the viscoelastic beam configuration shown in Fig. 1.

First, the time-dependent strain energy release rate, G_{a_1} , is obtained at increase of the right-hand crack at $0 \leq t \leq 1$. For this purpose, the balance of the energy is written as

$$M_p \delta \varphi_p + M_q \delta \varphi_q = \frac{\partial U}{\partial a_1} \delta a_1 + G_{a_1} h \delta a_1 \quad (26)$$

where M_p and M_q are the bending moments in the right-hand and left-hand crack arms, respectively, U is the time-dependent strain energy stored in the beam structure, δa_1 is a small increase of the right-hand crack. From (26), the strain energy release rate is derived as

$$G_{a_1} = \frac{M_p}{h} \frac{\partial \varphi_p}{\partial a_1} + \frac{M_q}{h} \frac{\partial \varphi_q}{\partial a_1} - \frac{1}{h} \frac{\partial U}{\partial a_1} \quad (27)$$

The time-dependent strain energy is found as

$$U = U_1 + U_2 + U_3 + U_4 \quad (28)$$

where U_1 , U_2 , U_3 and U_4 are the strain energies stored in the right-hand and left-hand crack arms, in portion, B_2B_3 , of the left-hand crack arm and in the un-cracked beam portion, $a_1 \geq x_5 \geq l$, respectively. It should be mentioned that formula (28) takes into account the fact that the interstitial crack arm is free of stresses.

The time dependent strain energy in the right-hand crack arm is written as

$$U_1 = a_1 b_1 \int_{-\frac{h}{2}}^{\frac{h}{2}} u_{01} dz_1 \quad (29)$$

where u_{01} is the time-dependent strain energy density in this crack arm, z_1 is the vertical centroidal axis of the cross-section of the crack arm (Fig. 3).

The time-dependent strain energy density is expressed as

$$u_{01} = \frac{1}{2} \sigma \varepsilon \quad (30)$$

The distribution of strains is treated by applying the hypothesis of Bernoulli for plane sections since beams of high length to height ratio are considered in the present paper.

Therefore, the distribution of strains along the height of the right-hand crack arm is written as

$$\varepsilon = \kappa_1 (z_1 - z_{1n}) \quad (31)$$

where

$$-\frac{h}{2} \leq z_1 \leq \frac{h}{2} \quad (32)$$

In formulae (31) and (32), κ_1 is the curvature of this crack arm, z_{1n} is the coordinate of the neutral axis.

By combining of (17), (30) and (31), one obtains

$$u_{01} = \frac{1}{2} \frac{\mu \kappa_1^2 (z_1 - z_{1n})^2}{\lambda t} (1 - e^{-\lambda t}) \quad (33)$$

The following approach is used to determine the curvature and the coordinate of the neutral axis. First, the angles of rotation of the free ends of the right-hand and left-hand crack arms are expressed as functions of the curvatures by using the integrals of Maxwell-Mohr

$$\varphi_p = \kappa_1 a_1 + \kappa_4 (l - a_1) \quad (34)$$

$$\varphi_q = \kappa_2 a_2 + \kappa_3 (a_1 - a_2) + \kappa_4 (l - a_1) \quad (35)$$

where κ_2 , κ_3 and κ_4 are the curvatures of left-hand crack arm, the portion, B_2B_3 , of the left-hand crack arm and the un-cracked portion of the beam, respectively. There are four unknowns, κ_1 , κ_2 , κ_3 and κ_4 , in Eqs. (34) and (35).

Four equations are written by using the fact that the axial forces in the right-hand crack arm, in portions, B_1B_2 and B_2B_3 , of the left-hand crack arm and in the un-cracked beam portion are equal to zero.

$$b_1 \int_{-\frac{h}{2}}^{\frac{h}{2}} \sigma dz_1 = 0 \quad (36)$$

$$b_3 \int_{-\frac{h}{2}}^{\frac{h}{2}} \sigma_\alpha dz_2 = 0 \quad (37)$$

$$(b_2 + b_3) \int_{-\frac{h}{2}}^{\frac{h}{2}} \sigma_\beta dz_3 = 0 \quad (38)$$

$$b \int_{-\frac{h}{2}}^{\frac{h}{2}} \sigma_\delta dz_4 = 0 \quad (39)$$

where σ_α , σ_β and σ_δ are the stresses in portions, B_1B_2 and B_2B_3 , of the left-hand crack arm and in the un-cracked beam portion, respectively, Z_2 , Z_3 and z_4 are the vertical centroidal axes of portions, B_1B_2 and B_2B_3 , of the left-hand crack arm and the un-cracked beam portion, respectively. The stress, σ_α , is found by replacing of ε with ε_α in (17) where ε_α is the strain in portion, B_1B_2 , of the left-hand crack arm. The distribution of ε_α is expressed by replacing of K_1 , Z_1 and Z_{1n} with K_2 , Z_2 and Z_{2n} in (31). Here, Z_{2n} is the coordinate of the neutral axis in portion, B_1B_2 , of the left-hand crack arm. Formula (17) is applied also obtain σ_β . For this purpose, ε is replaced with ε_β . In order to obtain the distribution of the strain, ε_β , the quantities, K_1 , Z_1 and Z_{1n} are replaced, respectively, with K_3 , Z_3 and Z_{3n} in (31) where Z_{3n} is the coordinate of neutral axis in portion, B_1B_2 , of the left-hand crack arm. The strain, ε , is replaced with δ_ε in (17) to obtain the stress, σ_δ , where ε_δ is the strain in the un-cracked beam portion. The distribution of ε_δ is found by replacing of K_1 , Z_1 and Z_{1n} with K_4 , Z_4 and Z_{1n} , respectively, in (31). Here Z_{4n} is the coordinate of neutral axis in the un-cracked beam portion.

One equation is obtained by considering the equilibrium of the bending moments in portions, B_1B_2 and B_2B_3 , of the left-hand crack arm

$$b_3 \int_{-\frac{h}{2}}^{\frac{h}{2}} \sigma_\alpha z_2 dz_2 = (b_2 + b_3) \int_{-\frac{h}{2}}^{\frac{h}{2}} \sigma_\beta z_3 dz_3 \quad (40)$$

Further one equation is written by using the fact that the sum of bending moments in the right-hand crack arm and in portion, B_2B_3 , of the left hand crack arm is equal to the bending moment in the un-cracked beam portion

$$b_1 \int_{-\frac{h}{2}}^{\frac{h}{2}} \sigma z_1 dz_1 + (b_2 + b_3) \int_{-\frac{h}{2}}^{\frac{h}{2}} \sigma_\beta z_3 dz_3 = b \int_{-\frac{h}{2}}^{\frac{h}{2}} \sigma_\delta z_4 dz_4 \quad (41)$$

After substituting of stresses in (36), (37), (38), (39), (40) and (41), these equations are solved together with (34) and (35) with respect to K_1 , K_2 , K_3 , K_4 , Z_{1n} , Z_{2n} , Z_{3n} and Z_{4n} at various values of time by using the MatLab computer program.

The time-dependent strain energy in portion, B_1B_2 , of the left-hand crack arm is obtained as

$$U_2 = a_2 b_3 \int_{-\frac{h}{2}}^{\frac{h}{2}} u_{02} dz_2 \quad (42)$$

where the time-dependent strain energy density, u_{02} , is found by replacing of K_1 , z_1 and z_{1n} with K_2 , Z_2 and Z_{2n} in (33).

The time-dependent strain energies stored in portion, B_2B_3 , of the left-hand crack arm and in the un-cracked beam portion are expressed as

$$U_3 = (a_1 - a_2)(b_2 + b_3) \int_{-\frac{h}{2}}^{\frac{h}{2}} u_{03} dz_3 \quad (43)$$

$$U_4 = (l - a_1)b \int_{-\frac{h}{2}}^{\frac{h}{2}} u_{04} dz_4 \quad (44)$$

where u_{03} and u_{04} are the time-dependent strain energy densities. The quantities, K_1 , Z_1 and Z_{1n} are replaced with K_3 , Z_3 and Z_{3n} , respectively, in (33) to derive u_{03} . The strain energy density, u_{04} , is obtained by replacing of K_1 , Z_1 and Z_{1n} with K_4 , Z_4 and Z_{4n} , respectively, in (33).

The bending moments, M_p and M_q , which are involved in the expression for the strain energy release rate (27) are obtained as

$$M_p = b_1 \int_{-\frac{h}{2}}^{\frac{h}{2}} \sigma_{z_1} dz_1 \quad (45)$$

$$M_q = b_3 \int_{-\frac{h}{2}}^{\frac{h}{2}} \sigma_{\alpha z_2} dz_2 \quad (46)$$

By substituting of in (28), (29), (34), (42), (43), (44), (45) and (46) in (27), one derives the following time-dependent solution to the strain energy release rate at increase of the right-hand crack arm:

$$G_{a_1} = \frac{b_1}{h} (\kappa_1 - \kappa_4) \int_{-\frac{h}{2}}^{\frac{h}{2}} \sigma_{z_1} dz_1 + \frac{b_3}{h} (\kappa_3 - \kappa_4) \int_{-\frac{h}{2}}^{\frac{h}{2}} \sigma_{\alpha z_2} dz_2 - \frac{1}{h} \left[b_1 \int_{-\frac{h}{2}}^{\frac{h}{2}} u_{01} dz_1 \right. \\ \left. - \frac{1}{h} \left[b_1 \int_{-\frac{h}{2}}^{\frac{h}{2}} u_{01} dz_1 + (b_2 + b_3) \int_{-\frac{h}{2}}^{\frac{h}{2}} u_{03} dz_3 - b \int_{-\frac{h}{2}}^{\frac{h}{2}} u_{04} dz_4 \right] \right] \quad (47)$$

The integration in (47) is performed by applying the MatLab Computer program. Formula (47) is used to calculate the strain energy release rate at various values of time. It should be noted that (47) is applicable at $0 \leq t \leq t_1$.

The strain energy release rate at increase of the right-hand crack is obtained also at $t \geq t_1$. For this purpose, (47) is applied. First, by combining of (20), (30) and (31), one derives the following expression for the time-dependent strain energy density in the right-hand crack arm:

$$u_{01} = \frac{1}{2} \zeta \kappa_1^2 (z_1 - z_{1n})^2 e^{\frac{E}{\eta_0}(t_1 - t)} \quad (48)$$

The curvatures and the coordinates of the neutral axes in the right-hand crack arm, in portions, B_1B_2 and B_2B_3 , of the left-hand crack arm and in the un-cracked beam portion are determined by applying equations (34), (35), (36), (37), (38), (39), (40) and (41). For this purpose, the stress in the right-hand crack arm is obtained by (20). The stresses, σ_α , σ_β and σ_δ , are found by replacing of ε with ε_α , ε_β and ε_δ respectively, in (20).

Formula (48) is applied also to derive the time-dependent strain energy density in portion, B_1B_2 , of the left-hand crack arm by replacing of K_1 , Z_1 and Z_{1n} with K_2 , Z_2 and Z_{2n} , respectively.

The time-dependent strain energy density in portion, B_3B_3 , of the left-hand crack arm is found by (48). For this purpose, K_1 , Z_1 and Z_{1n} are replaced with K_3 , Z_3 and Z_{3n} , respectively.

The quantities, K_1 , Z_1 and Z_{1n} are replaced with K_4 , Z_4 and Z_{4n} , respectively, in (48) to calculate the time-dependent strain energy density in the un-cracked beam portion.

Finally, after substituting of the stresses and the time-dependent strain energy densities in (47), the strain energy release rate is calculated at various values of time (the integration is carried-out by using the MatLab computer program).

The time-dependent strain energy release rate is derived also at increase of the left-hand crack arm. For this purpose, α_1 is replaced with α_2 in (27). First, a solution to the strain energy release rate is obtained at $0 \leq t \leq t_1$. By combining of (27), (28), (29), (34), (42), (43), (44), (45) and (46), one derives

$$G_{a_2} = \frac{b_3}{h} (\kappa_2 - \kappa_3) \int_{-\frac{h}{2}}^{\frac{h}{2}} \sigma_\alpha z_2 dz_2 - \frac{1}{h} \left[b_3 \int_{-\frac{h}{2}}^{\frac{h}{2}} u_{02} dz_2 - (b_2 + b_3) \int_{-\frac{h}{2}}^{\frac{h}{2}} u_{03} dz_3 \right] \quad (49)$$

The MatLab computer program is used to carry-out the integration in (49). Formula (49) is applied to calculate the strain energy release rate at various values of time.

The time-dependent strain energy release rate at increase of the left-hand crack is found also at $t \geq t_1$. For this purpose, the stress, σ_α , obtained by replacing of ε with ε_α in (20), and the time-dependent strain energy densities, u_{02} and u_{03} , obtained by performing the necessary replacements in (48), are substituted in (49). Calculations of the strain energy release rate by (49) are carried-out at various values of time.

Time-dependent solutions to the strain energy release rate are derived also by differentiating of the time-dependent strain energy with respect to the crack area. First, a solution is obtained at increase of the right-hand crack at $0 \leq t \geq t_1$. For this purpose, the strain energy release rate is written as

$$G_{a_1} = \frac{dU}{hda_1} \quad (50)$$

By substituting of (28), (29), (42), (43) and (44) in (50), one derives

$$G_{a_1} = \frac{1}{h} \left[b_1 \int_{-\frac{h}{2}}^{\frac{h}{2}} u_{01} dz_1 + (b_2 + b_3) \int_{-\frac{h}{2}}^{\frac{h}{2}} u_{03} dz_3 - b \int_{-\frac{h}{2}}^{\frac{h}{2}} u_{04} dz_4 \right] \tag{51}$$

where the time-dependent strain energy density, u_{01} , is found by using (33). The time-dependent strain energy densities, u_{02} and u_{03} , are obtained by performing the necessary replacements in (33). Formula (51) is applied to calculate the strain energy release rate at various values of time. It should be mentioned that the strain energy release rate found by (51) is exact match of that obtained by using (47). This fact proves the correctness of the solutions derived.

The time-dependent strain energy release rate at increase of the right-hand crack is found also at $t \geq t_1$. For this purpose, the time-dependent strain energy densities obtained by using formula (48) are substituted in (51). Calculations of the strain energy release rate are performed at various values of time. The results obtained match exactly these found by considering the balance of the energy.

In order to derive the time-dependent strain energy release rate at increase of the left-hand crack, formula (51) is re-written as

$$G_{a_2} = \frac{dU}{hda_2} \tag{52}$$

First, a solution is obtained at $0 \leq t \leq t_1$. For this purpose, (28), (29), (42), (43) and (44) are substituted in (52). The result is

$$G_{a_2} = \frac{1}{h} \left[b_3 \int_{-\frac{h}{2}}^{\frac{h}{2}} u_{02} dz_2 - (b_2 + b_3) \int_{-\frac{h}{2}}^{\frac{h}{2}} u_{03} dz_3 \right] \tag{53}$$

where the time-dependent strain energy densities are found by using (48). By applying (53), the strain energy release rate is calculated at various values of time (the integration is carried-out by

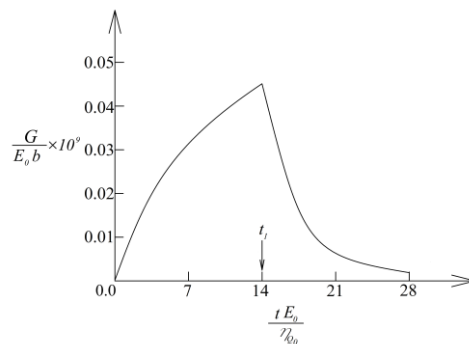


Fig. 4 The strain energy release rate in non-dimensional form presented as a function of the non-dimensional time for the right-hand crack

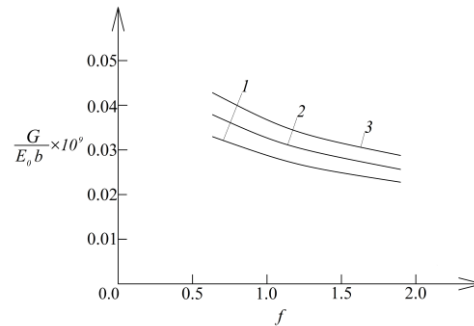


Fig. 5 The strain energy release rate in non-dimensional form presented as a function of f for the right-hand crack (curve 1 – at $b_1/b=0.1$, curve 2 - at $b_1/b=0.2$ and curve 3 - at $b_1/b=0.3$)

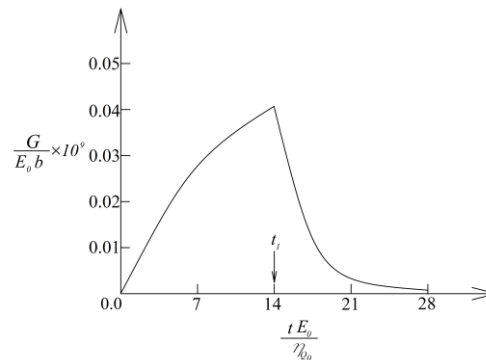


Fig. 6 The strain energy release rate in non-dimensional form presented as a function of the non-dimensional time for the left-hand crack

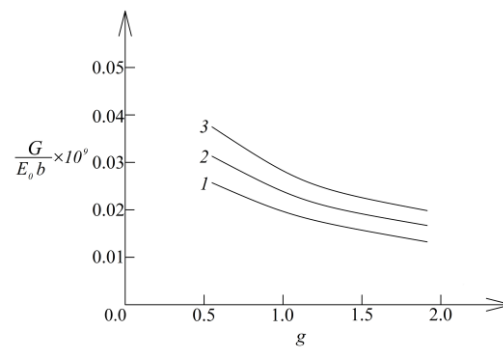


Fig. 7 The strain energy release rate in non-dimensional form presented as a function of g for the left-hand crack (curve 1 – at $b_3/b_1=0.15$, curve 2 – at $b_3/b_1=0.30$ and curve 3 – at $b_3/b_1=0.45$)

the MatLab computer program). The strain energy release rate found by (53) is exact match of that obtained by (49) which is prove for correctness of the solutions.

Formula (53) is applied also to calculate the time-dependent strain energy release rate at increase of the left-hand crack at $t \geq t_1$. In this case, the time-dependent strain energy densities which are

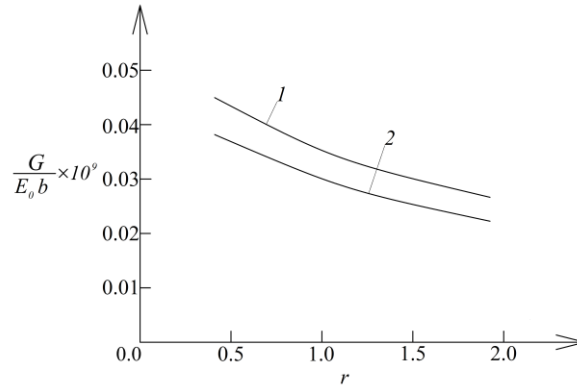


Fig. 8 The strain energy release rate in non-dimensional form presented as a function of parameter, r (curve 1 – for the right-hand crack and curve 2 – for the left-hand crack)

involved in (53) are found by using (49). It should be noted that the strain energy release rate calculated by (53) is exact match of that derived by considering the balance of the energy at increase of the left-hand crack at $t \geq t_1$.

4. Parametric analysis

A parametric analysis of the time-dependent strain energy release rates for the longitudinal cracks in the viscoelastic inhomogeneous cantilever beam shown in Fig. 1 is carried-out. For this purpose, calculations are performed by applying the solutions derived in section 3 of this paper. The strain energy release rate is expressed in non-dimensional form by using the formula $G_N = G/(E_0 b)$. One of the aims of the parametric analysis is to evaluate the change of the strain energy release rate with time. The influences of the continuous material inhomogeneity and the locations of the cracks along the width of the beam on the strain energy release rate are assessed too. It is assumed that $b=0.010$ m, $h=0.015$ m, $\nu_p=0.12 \times 10^{-7}$ rad/sec and $\nu_q=0.10 \times 10^{-7}$ rad/sec.

In order to evaluate the change of the strain energy release rate with time, first, calculations are carried-out by applying the solutions derived at increase of the right-hand crack. The results obtained are shown in Fig. 4 where the strain energy release rate in non-dimensional form is presented as a function of the non-dimensional time. The time is expressed in non-dimensional form by applying the formula $t_N = tE_0/\eta_{Q0}$. The curve in Fig. 4 indicates that the strain energy release rate increases at $0 \leq t \leq t_1$ (this finding is attributed to the increase of the angles of rotation of the free ends of the right-hand and left-hand crack arms). One can observe also in Fig. 4 that the strain energy release rate decreases at $t \geq t_1$ (this behavior is due to stress relaxation at constant applied strain at $t \geq t_1$).

The influence of the continuous variation of the modulus of elasticity along the height of the beam on the strain energy release rate is investigated. For this purpose, calculations are performed at various values of parameter, f , by applying the solution of the strain energy release rate for the right-hand crack. The influence of the location of the right-hand crack along the width of the beam on the strain energy release rate is investigated by calculating of the strain energy release rate at various b_1/b ratios.

One can get an idea about the influence of the variation of the modulus of elasticity and the location of the crack on the strain energy release rate from Fig. 5 where the strain energy release rate in non-dimensional form is presented as a function of f at three b_1/b ratios.

It can be observed in Fig. 5 that the strain energy release rate decreases with increasing of f . The curves in Fig. 5 show also that the strain energy release rate increases with increasing of b_1/b ratio.

The change of the strain energy release rate with time is assessed also for the left-hand crack.

The strain energy release rate calculated by using the solutions derived at increase of the left-hand crack is presented in non-dimensional form as a function of the non-dimensional time in Fig. 6.

It can be observed in Fig. 6 that the strain energy release rate increases with time at $0 \leq t \leq t_1$. At $t \geq t_1$, the strain energy release rate decreases with time (Fig. 6).

The effect of the continuous variation of the coefficient of viscosity, η_Q , along the height of the beam and the location of the left-hand crack along the beam width on the strain energy release rate is studied by carrying-out calculations of the strain energy release rate at various values of parameter, g , and various b_3/b_1 ratios (the b_3/b_1 ratio characterizes the location of the left-hand crack along the beam width). The strain energy release rate in non-dimensional form is presented as a function of g in Fig. 7 at three b_3/b_1 ratios. It is evident from Fig. 7 that the strain energy release rate increases with increasing of b_3/b_1 ratio. The curves in Fig. 7 indicate also that the strain energy release rate decreases with increasing of g .

The influence of the continuous variation of η_R along the height of the beam on the strain energy release rate is illustrated in Fig. 8 where the strain energy release rate calculated by using the solutions (47) and (53) is presented in non-dimensional form as a function of parameter, r . It can be observed in Fig. 8 that the increase of r leads to decrease of the strain energy release rate. One can observe also in Fig. 8 that the strain energy release rate for the left-hand crack is lower than that for the right-hand crack.

5. Conclusions

An analytical study of two longitudinal vertical cracks in a viscoelastic continuously inhomogeneous cantilever beam structure is developed. A viscoelastic model with one linear spring and two linear dashpots is used for describing the mechanical behavior of the beam. The viscoelastic model is under strain that increases at a constant speed with time up to a given magnitude and then the strain remains constant. Stress-strain-time relationships of the viscoelastic model are derived for both stages (at increasing strain and at constant strain). The modulus of elasticity of the spring and the coefficients of viscosity of the two dashpots of the viscoelastic model vary continuously along the height of the beam since the beam is continuously inhomogeneous along its height. The two longitudinal cracks are located arbitrary along the width of the beam. Solutions to the time-dependent strain energy release rate which take into account the viscoelastic behavior of the continuously inhomogeneous material are derived for both cracks. For this purpose, the balance of the energy is analyzed. The strain energy stored in the beam is obtained by integrating of the time-dependent strain energy density. The time-dependent strain energy release rate is found for both stages (at increasing strain with time and at constant strain). Solutions to the time-dependent strain energy release rate are obtained also by differentiating of the time-dependent strain energy with respect to the crack area. The two solutions produce identical results which prove their correctness. The change of the strain energy release rate with

time is analyzed. The analysis reveals that the strain energy release rate increases with time at the first stage of loading (when the strain increases at constant speed). At the second stage of loading, when the strain remains constant with time, the strain energy release rate decreases with time (this is due to the stress relaxation under constant applied strain). The influence of the continuous material inhomogeneity on the strain energy release rate is evaluated. It is found that the strain energy release rate decreases with increasing of f , g and r . Concerning the effect of the locations of the two cracks along the width of the beam, the calculations indicate that the strain energy release rate increases with increasing of b_1/b and b_3/b ratios. The analysis shows that the strain energy release rate for the right-hand crack is higher than that for the left-hand crack. The findings of the present study clearly indicate that the strain energy release rate for longitudinal vertical cracks in viscoelastic continuously inhomogeneous beam structures depends to a great extent on the character of the variation of the strains with time. Therefore, the variation of the strains with time has to be considered in fracture mechanics based preliminary structural design of inhomogeneous members and components which exhibit viscoelastic behavior.

References

- Akbulut, M. and Sonmez, F.O. (2008), "Optimum design of composite laminates for minimum thickness", *Comput. Struct.*, **86**(21-22), 1974-1982. <https://doi.org/10.1016/j.compstruc.2008.05.003>.
- Akbulut, M., Sarac, A. and Ertas, A.H. (2020), "An investigation of non-linear optimization methods on composite structures under vibration and buckling loads", *Advan. Comput. Des.*, **5**(3), 209-231. doi.org/10.12989/acd.2020.5.3.209
- Altunsaray, E. (2017), "Static deflections of symmetrically laminated quasi-isotropic super-elliptical thin plates", *Ocean Eng.*, **141**(1), 337-350. <https://doi.org/10.1016/j.oceaneng.2017.06.032>.
- Altunsaray, E. and Bayer, İ. (2014), "Buckling of symmetrically laminated quasi-isotropic thin rectangular plates", *Steel Compos. Struct.*, **17**(3), 305-320. <https://doi.org/10.12989/scs.2014.17.3.305>.
- Altunsaray, E., Ünsalan, D., Nesar, G., Turgut, Gürsel, K.T. and Taner, M. (2019), "Parametric study for static deflections of symmetrically laminated rectangular thin plates", *Sci. Bull. Mircea cel Batran Naval Academy*, Constanta, **22**(1), 1-12. [10.21279/1454-864X-19-11-041](https://doi.org/10.21279/1454-864X-19-11-041).
- Butcher, R.J., Rousseau, C.E. and Tippur, H.V. (1999), "A functionally graded particulate composite: Measurements and failure analysis", *Acta. Mater.*, **47**(2), 259-268. [https://doi.org/10.1016/S1359-6454\(98\)00305-X](https://doi.org/10.1016/S1359-6454(98)00305-X).
- Dolgov, N.A. (2002), "Effect of the elastic modulus of a coating on the serviceability of the substrate-coating system", *Strength Mater.*, **37**(2), 422-431. <https://doi.org/10.1007/s11223-005-0053-7>.
- Dolgov, N.A. (2005), "Determination of stresses in a two-layer coating", *Strength Mater.*, **37**(2), 422-431. <https://doi.org/10.1007/s11223-005-0053-7>.
- Dolgov, N.A. (2016), "Analytical methods to determine the stress state in the substrate-coating system under mechanical loads", *Strength Mater.*, **48**(1), 658-667. <https://doi.org/10.1007/s11223-016-9809-5>.
- Gasik, M.M. (2010), "Functionally graded materials: bulk processing techniques", *Int. J. Mater. Product Technol.*, **39**(1-2), 20-29. <https://doi.org/10.1504/IJMPT.2010.034257>.
- Hedia, H.S., Aldousari, S.M., Abdellatif, A.K. and Fouda, N.A. (2014), "New design of cemented stem using functionally graded materials (FGM)", *Biomed. Mater. Eng.*, **24**(3), 1575-1588. [10.3233/BME-140962](https://doi.org/10.3233/BME-140962).
- Hirai, T. and Chen, L. (1999), "Recent and prospective development of functionally graded materials in Japan", *Mater. Sci. Forum*, **308-311**(4), 509-514. <https://doi.org/10.4028/www.scientific.net/MSF.308-311.509>.
- Mahamood, R.M. and Akinlabi, E.T. (2017), *Functionally Graded Materials*, Springer.
- Markworth, A.J., Ramesh, K.S. and Parks, Jr. W.P. (1995), "Review: modeling studies applied to functionally graded materials", *J. Mater. Sci.*, **30**(3), 2183-2193. <https://doi.org/10.1007/BF01184560>.

- Miyamoto, Y., Kaysser, W.A., Rabin, B.H., Kawasaki, A. and Ford, R.G. (1999), *Functionally Graded Materials: Design, Processing and Applications*, Kluwer Academic Publishers, Dordrecht/London/Boston.
- Nemat-Allal, M.M., Ata, M.H., Bayoumi, M.R. and Khair-Eldeen, W. (2011), "Powder metallurgical fabrication and microstructural investigations of Aluminum/Steel functionally graded material", *Mater. Sci. Appl.*, **2**(5), 1708-1718. 10.4236/msa.2011.212228.
- Rezaiee-Pajand, M. and Hozhabrossadati, S.M. (2016), "Analytical and numerical method for free vibration of double-axially functionally graded beams", *Compos. Struct.*, **152**, 488-498. doi.org/10.1016/j.compstruct.2016.05.003.
- Rezaiee-Pajand, M., Masoodi, A.R. and Mokhtari, M. (2018), "Static analysis of functionally graded non-prismatic sandwich beams", *Advan. Comput. Des.*, **3**(2), 165-190. http://dx.doi.org/10.12989/acd.2018.3.2.165.
- Rezaiee-Pajand, M., Sani, A.A. and Hozhabrossadati, S.M. (2017), "Application of differential transform method to free vibration of gabled frames with rotational springs", *Int. J. Struct. Stab. Dynam.*, **17**(1), 1750012. doi.org/10.1142/S0219455417500122.
- Rizov, V.I. (2017), "Analysis of longitudinal cracked two-dimensional functionally graded beams exhibiting material non-linearity", *Frattura ed Integrità Strutturale*, **41**, 498-510. https://doi.org/10.3221/IGF-ESIS.41.61
- Rizov, V.I. (2018), "Non-linear fracture in bi-directional graded shafts in torsion", *Multidiscipline Modeling Mater. Struct.*, **15**(1), 156-169. https://doi.org/10.1108/MMMS-12-2017-0163.
- Rizov, V.I. (2020), "Longitudinal fracture analysis of inhomogeneous beams with continuously changing radius of cross-section along the beam length", *Strength, Fracture Complexity: Int. J.*, **13**, 31-43. 10.3233/SFC-200250.
- Tokovyy, Y. (2019), "Solutions of axisymmetric problems of elasticity and thermoelasticity for an inhomogeneous space and a half space", *J. Mathemat. Sci.*, **240**(1), 86-97. https://doi.org/10.1007/s10958-019-04337-3.
- Tokovyy, Y. and Ma, C.C. (2017), "Three-dimensional elastic analysis of transversely-isotropic composites", *J. Mech.*, **33**(6), 821-830. https://doi.org/10.1017/jmech.2017.91.
- Tokovyy, Y. and Ma, C.C. (2019), "Elastic analysis of inhomogeneous solids: History and development in brief", *J. Mech.*, **18**(1), 1-14. https://doi.org/10.1017/jmech.2018.57.
- Uslu Uysal, M. (2016), "Buckling behaviours of functionally graded polymeric thin-walled hemispherical shells", *Steel Compos. Struct.*, **21**(1), 849-862. https://doi.org/10.12989/scs.2016.21.4.849.
- Uslu Uysal, M. and Güven, U. (2015), "Buckling of functional graded polymeric sandwich panel under different load cases", *Compos. Struct.*, **121**, 182-196. https://doi.org/10.1016/j.compstruct.2014.11.012.
- Uslu Uysal, M. and Güven, U. (2016), "A bonded plate having orthotropic inclusion in adhesive layer under in-plane shear loading", *J. Adhesion*. **92**, 214-235. https://doi.org/10.1080/00218464.2015.1019064.
- Uslu Uysal, M. and Kremzer, M. (2015), "Buckling behaviour of short cylindrical functionally gradient polymeric materials", *Acta Physica Polonica*, **A127**, 1355-1357. 10.12693/APhysPolA.127.1355.